




Spatiotemporal coupled-mode equations for arbitrary pulse transformation

Zhaohui Dong ¹, Xianfeng Chen,^{1,2,3} and Luqi Yuan ^{1,*}

¹State Key Laboratory of Advanced Optical Communication Systems and Networks, School of Physics and Astronomy, Shanghai Jiao Tong University, Shanghai 200240, People's Republic of China

²Shanghai Research Center for Quantum Sciences, Shanghai 201315, People's Republic of China

³Collaborative Innovation Center of Light Manipulation and Applications, Shandong Normal University, Jinan 250358, People's Republic of China

 (Received 1 June 2023; revised 6 October 2023; accepted 12 October 2023; published 13 November 2023)

Spatiotemporal modulation offers a variety of opportunities for light manipulations. In this paper, we propose a way toward arbitrary transformation for pulses sequentially propagating within one waveguide in space via temporal waveguide coupling. The temporal waveguide coupling operation is achieved by spatiotemporally modulating the refractive index of the spatial waveguide with a traveling wave through segmented electrodes. We derive the temporal coupled-mode equations and discuss how systematic parameters affect the temporal coupling coefficients. We further demonstrated a temporal Mach-Zehnder interferometer and universal multiport interferometer, which enables arbitrary unitary transformation for pulses. We showcase a universal approach for transforming pulses among coupled temporal waveguides, which requires only one spatial waveguide under spatiotemporal modulation, and hence provide a flexible, compact, and highly compatible method for optical signal processing in time domain.

DOI: [10.1103/PhysRevResearch.5.043150](https://doi.org/10.1103/PhysRevResearch.5.043150)

I. INTRODUCTION

Time-varying media brings intriguing opportunities for wave manipulation in photonics [1–5] and hence attracts growing interest in both physics community and optical engineering. In particular, by combining both temporal and spatial degrees of freedom, the photonic systems undergoing spatiotemporal modulations recently emerge as new platforms for controlling light simultaneously in space and time [6–11]. Utilizing this powerful approach, researchers explore many exotic phenomena which cannot be realized in a static medium, such as luminal amplification [12–14], Fresnel drag [15,16], magnet-free nonreciprocal systems [17–19], and temporal double-slit interference [20]. As an outstanding example of spatiotemporally modulated systems, a temporal waveguide which harnesses the total internal reflection of light at spatiotemporal boundaries, and therefore confines pulses in between [21,22], provides a novel concept for guiding light. Up to date, previous research on temporal waveguides focus on fundamental properties for realizing a single temporal waveguide [22,23], while interactions between multiple temporal waveguides remain unexplored. Moreover, the spatiotemporally modulated system may not be described by the spatial coupled-mode theory [24,25], so it desires a relevant

theoretical formalism to model the spatiotemporally coupled modes in a proper way.

In this paper, we extend the spatial coupled-mode theory to temporal waveguide regime, and derive the fundamental formula for modeling interactions between two temporal waveguides, i.e., the spatiotemporal coupled-mode theory. Systematic parameters which determine temporal coupling coefficients are given, and hence our theory introduces a basic framework for studying the problem of coupled temporal waveguides. To showcase the capability of our formalism, we explore a temporal Mach-Zehnder interferometer (MZI) and further propose a design of a universal multiport interferometer [26–29] in the time domain for optical pulses. Such a universal multiport interferometer enables an arbitrary temporal transformation for sequential-propagating pulses within one spatial waveguide under the spatiotemporal modulation, which could find potential applications in optical signal processing. Our work hence provides a useful theoretical tool in the arising field of spatiotemporal metamaterials [1–5,30] to develop new-generation active photonic devices.

II. MODEL

We now start to show how to model interactions between two temporal waveguides and derive the coupled-mode formula in the time domain. Before getting into details, we first review the model of a temporal waveguide which is achieved with pulse propagating in a spatiotemporally modulated waveguide as shown in Fig. 1(a). The modulation of the refractive index of the waveguide is chosen as $n(z, t) = n_0 + \xi(z - v_B t)$, where n_0 is the background refractive index of the waveguide and $\xi(z - v_B t)$ denotes the spatiotemporal change of the refractive index [22] with z being the propagating

*yuanluqi@sjtu.edu.cn

Published by the American Physical Society under the terms of the [Creative Commons Attribution 4.0 International license](https://creativecommons.org/licenses/by/4.0/). Further distribution of this work must maintain attribution to the author(s) and the published article's title, journal citation, and DOI.

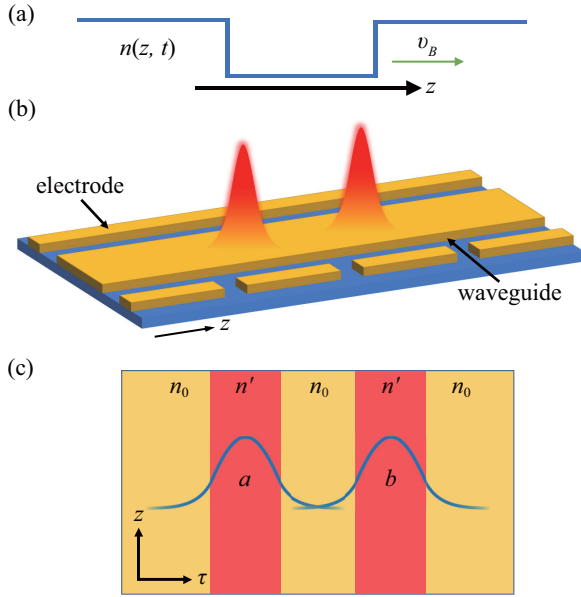


FIG. 1. (a) Schematic of the spatiotemporal modulation of the refractive index in a waveguide to achieve a temporal waveguide. (b) Scheme of the interaction of temporal waveguides, which is based on a waveguide modulated by traveling-wave signals through electrode arrays. (c) Refraction index $n(z, \tau)$ and fundamental modes $M(\tau)$ in blue curves of the temporal waveguide a and b in the retarded frame (z, τ) . Here $n' = n_0 + \Delta n$.

direction, and v_B being the moving speed of the modulation. We transfer the formalism in a retarded time frame by using the transformation $\tau = t - z/v_B$, where t is the time in the laboratory frame. In the retarded time frame (z, τ) , the change of the refractive index $\xi(z - v_B t)$ is transformed to a z independent function $\xi(\tau) = \xi_0 + \Delta\xi(\tau)$. To achieve a temporal waveguide, $\xi(\tau)$ can be chosen as

$$\xi(\tau) = \begin{cases} \Delta n & |\tau - \tau_c| \leq T_w/2, \\ 0 & |\tau - \tau_c| > T_w/2, \end{cases} \quad (1)$$

where Δn is the modulation amplitude, and T_w is the modulation time width centered at τ_c in the time retarded frame. As an analog to the conventional spatial waveguide, one can consider $|\tau - \tau_c| \leq T_w/2$ as the core region of the temporal waveguide, and $|\tau - \tau_c| > T_w/2$ as the cladding region.

We then consider a pulse having a central frequency ω_0 propagates along such spatiotemporally modulated waveguide with the modulation format in Eq. (1). One can treat such a problem by Taylor expanding the dispersion relation of the waveguide as [21,22]

$$\beta(\omega) = \beta_0 + \Delta\beta_1(\omega - \omega_0) + \frac{\beta_2}{2}(\omega - \omega_0)^2 + \beta_m(\tau), \quad (2)$$

where $\beta_0 = n_0\omega_0/c$ and $\Delta\beta_1 = \beta_1 - 1/v_B$ with $\beta_1 = \partial\beta/\partial\omega|_{\omega_0}$ being the reciprocal of the group velocity at ω_0 , $\beta_2 = \partial^2\beta/\partial\omega^2|_{\omega_0}$ being the corresponding group velocity dispersion, and $\beta_m(\tau) = \beta_0 \xi(\tau)/n_0$ represents the change of the propagation constant due to spatiotemporal modulation. By using Maxwell's equation and the dispersion relation in Eq. (2), one obtains the resulting wave equation for describing

the amplitude of propagating pulse $A(z, \tau)$ in the retarded frame (for detailed derivation see Appendix A):

$$\frac{\partial A(z, \tau)}{\partial z} + \Delta\beta_1 \frac{\partial A(z, \tau)}{\partial \tau} + i \frac{\beta_2}{2} \frac{\partial^2 A(z, \tau)}{\partial \tau^2} = i\beta_m(\tau)A(z, \tau). \quad (3)$$

Following the treatment in Ref. [22], one can take the modal solution $A(z, \tau)$ as $A(z, \tau) = M(\tau)\exp[i(Kz - \Omega\tau)]$, where $M(\tau)$ describes the spatiotemporal shape of the mode, K denotes the rate of the mode accumulating phase during propagation, and $\Omega = -\Delta\beta_1/\beta_2$ is the frequency shift. So far, we briefly outline the formalism of the optical pulse propagating in a waveguide under the spatiotemporal modulation of the refractive index, i.e., the field traveling inside a temporal waveguide in the retarded frame, which has been utilized in many follow-up studies [22,23,31,32].

Next we give the important formula of the spatiotemporal coupled-mode theory. We construct two temporal waveguides (labeled as a and b), which is achieved by spatiotemporally modulating the refractive index of a spatial waveguide through the traveling-wave signal by segmented electrodes as shown in Fig. 1(b). In particular, the spatiotemporal change of the refractive index in the retarded time frame is taken as

$$\xi'(\tau) = \xi_0 + \Delta\xi_a(\tau) + \Delta\xi_b(\tau), \quad (4)$$

where $\Delta\xi_a(\tau)$ and $\Delta\xi_b(\tau)$ follow Eq. (1) centered at τ_c^a and τ_c^b ($|\tau_c^b - \tau_c^a| > T_w$), and therefore form two temporal waveguides a and b in Fig. 1(c), respectively.

We consider the field at the central frequency ω_0 propagating in such a spatiotemporally modulated waveguide and assume a solution as

$$A(z, \tau) = G_a(z)M_a(\tau)\exp[i(K_a z - \Omega\tau)] + G_b(z)M_b(\tau)\exp[i(K_b z - \Omega\tau)], \quad (5)$$

where G_a (G_b) represents the envelope amplitude of the pulse in the temporal waveguide a (b), and the corresponding modal distribution $M_i(\tau)$ and $K_i(\tau)$ ($i = a, b$) satisfy [22]

$$\frac{\partial^2 M_i(\tau)}{\partial \tau^2} + \frac{2}{\beta_2} \left[K_i + \frac{(\Delta\beta_1)^2}{2\beta_2} - \beta_m^i(\tau) \right] M_i(\tau) = 0, \quad (6)$$

where $\beta_m^i(\tau) = \beta_0 \xi_i(\tau)/n_0$. Substituting Eq. (5) into Eq. (3), multiplying by $M_a^*(\tau)$ or $M_b^*(\tau)$, and then integrating over τ , we obtain the temporal coupled-mode equations:

$$\begin{aligned} \frac{\partial G_a(z)}{\partial z} &= i \frac{\kappa_{ab} - C_{ab}\gamma_{ba}}{1 - C_{ab}C_{ba}} \exp[i(K_b - K_a)z] G_b(z) \\ &\quad + i \frac{\gamma_{ab} - C_{ab}\kappa_{ba}}{1 - C_{ab}C_{ba}} G_a(z), \end{aligned} \quad (7a)$$

$$\begin{aligned} \frac{\partial G_b(z)}{\partial z} &= i \frac{\kappa_{ba} - C_{ba}\gamma_{ab}}{1 - C_{ba}C_{ab}} \exp[-i(K_b - K_a)z] G_a(z) \\ &\quad + i \frac{\gamma_{ba} - C_{ba}\kappa_{ab}}{1 - C_{ba}C_{ab}} G_b(z), \end{aligned} \quad (7b)$$

where C_{ij} , κ_{ij} , and γ_{ij} ($i \neq j$) are expressed as

$$C_{ij} = \int M_i^*(\tau)M_j(\tau)d\tau / \int M_i^*(\tau)M_i(\tau)d\tau, \quad (8a)$$

$$\kappa_{ij} = \int M_i^*(\tau)\Delta\beta_m^i(\tau)M_j(\tau)d\tau / \int M_i^*(\tau)M_i(\tau)d\tau, \quad (8b)$$

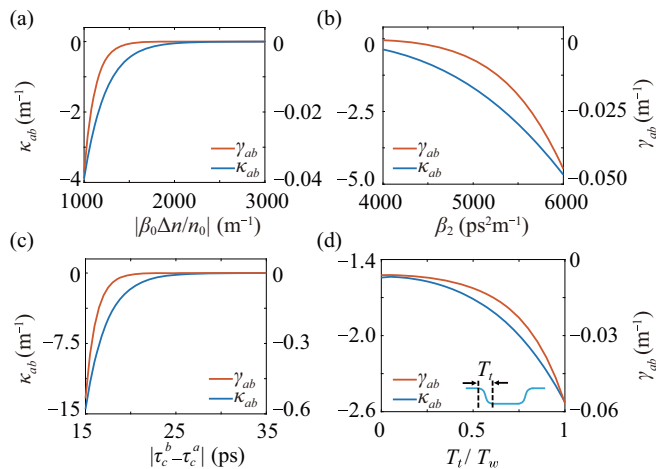


FIG. 2. γ_{ab} and κ_{ab} versus (a) $|\beta_0 \Delta n/n_0|$, (b) β_2 , (c) time spacing between two temporal waveguides, and (d) turn-on/off time width T_t .

$$\gamma_{ij} = \int M_i^*(\tau) \Delta \beta_m^j(\tau) M_i(\tau) d\tau / \int M_i^*(\tau) M_i(\tau) d\tau, \quad (8c)$$

and $\Delta \beta_m^i(\tau) = \beta_0 \Delta \xi_i(\tau)/n_0$. If we further assume the two temporal waveguides are identical in temporal shapes and $\int M_i^*(\tau) M_j(\tau) d\tau \ll \int M_i^*(\tau) M_i(\tau) d\tau$, we get $K_a = K_b$ and $C_{ab} \approx C_{ba} \approx 0$. Equations (7a) and (7b) can then be simplified as

$$\frac{\partial G_a(z)}{\partial z} \approx i\kappa_{ab} G_b(z) + i\gamma_{ab} G_a(z), \quad (9a)$$

$$\frac{\partial G_b(z)}{\partial z} \approx i\kappa_{ba} G_a(z) + i\gamma_{ba} G_b(z). \quad (9b)$$

where T_t denotes the turn-on/off time width between the temporal core and the cladding regions [see the subfigure in Fig. 2(d)]. One can find that in Fig. 2(d), when T_t/T_w becomes larger, γ_{ab} and κ_{ab} are increasing, indicating that the confinement of the pulse is weaker. Nevertheless, when $T_t \sim 10\% T_w$, both coefficients do not change much compared to those when $T_t = 0$, i.e., the ideal modulation case. Therefore, in the following, we still simulate models under the ideal modulation case. The approximation we make here might become unrealistic when the spatiotemporal modulation of the refractive index $\Delta \xi(\tau)$ becomes too large which cannot be taken as a perturbation.

III. RESULTS

So far, we derive the spatiotemporal coupled-mode equations for modeling interactions between two temporal waveguides and investigate how systematic parameters of the system affect temporal coupling coefficients. In the following, we use

Here, κ_{ij} is the temporal coupling coefficient, and γ_{ij} is the shift due to the presence of the other temporal waveguide. Note that we consider a symmetry case here, so we can take $\kappa_{ij} = \kappa_{ji}^*$ and $\gamma_{ab} = \gamma_{ba}$. We explain the coupling of temporal waveguides in Appendix C.

To give an illustrative picture on how the systematic parameters of this spatiotemporally modulated waveguide determine the coefficients in the temporal coupled-mode equations (9), we give an example with experimentally feasible parameters. We choose $\beta_0 \Delta n/n_0 = -1200 \text{ m}^{-1}$, $\Delta \beta_1 = 0$, and $\beta_2 = 5000 \text{ ps}^2 \text{ m}^{-1}$, which are standard parameters for an optical waveguide with the modulation strength $\Delta n/n_0 \sim 10^{-4}$ [33–35]. The spatiotemporal modulation shape can take $T_w = 10 \text{ ps}$, and $|\tau_c^b - \tau_c^a| = 20 \text{ ps}$. We now tune one of these parameters and fix others to investigate how γ_{ab} and κ_{ab} are affected. Only the coupling between fundamental modes is considered, where corresponding mathematical expressions are given in Appendix B. We first change $|\beta_0 \Delta n/n_0|$ as shown in Fig. 2(a). The role of $|\beta_0 \Delta n/n_0|$ in temporal waveguides is similar to the index contrast between the core region and cladding region in spatial waveguides. When $|\beta_0 \Delta n/n_0|$ becomes larger, both γ_{ab} and κ_{ab} become weaker. Next we vary the dispersion parameter β_2 , which describes the ability of light to spread out of the core region in the temporal waveguide. As a result, a larger β_2 results in larger γ_{ab} and κ_{ab} as shown in Fig. 2(b). Figure 2(c) shows changes of γ_{ab} and κ_{ab} versus the time spacing between two temporal waveguides $|\tau_c^b - \tau_c^a|$, and one can see both coefficients decrease when the time spacing increases as two temporal waveguides fall apart in the time domain. In all calculations above, we consider the ideal modulations, i.e., the change of $\Delta \beta_m^i(\tau)$ is abrupt. In reality, the turn on/off of modulations is not instantaneous. To reflect this feature, we consider the form of $\Delta \beta_m^i(\tau)$ as

$$\Delta \beta_m^i(\tau) = \begin{cases} \beta_0 \Delta n/n_0 & |\tau - \tau_c^i| < \frac{1}{2}(T_w - T_t), \\ \beta_0 \Delta n/n_0 \cos[|\tau - \tau_c^i| - \frac{1}{2}(T_w - T_t)] & \frac{1}{2}(T_w - T_t) \leq |\tau - \tau_c^i| < \frac{1}{2}(T_w + T_t), \\ 0 & \text{others,} \end{cases} \quad (10)$$

these equations and demonstrate a temporal MZI with parameters $\beta_0 \Delta n/n_0 = -1200 \text{ m}^{-1}$, $\Delta \beta_1 = 0$, $\beta_2 = 5000 \text{ ps}^2 \text{ m}^{-1}$, and $T_w = 10 \text{ ps}$. The scheme of such temporal MZI is depicted in Fig. 3(a), with values of $\beta_m(z, \tau) = 1200 \text{ m}^{-1}$ in the cyan regime and $= 0 \text{ m}^{-1}$ in the orange regime of the retarded frame (τ, z) . The input and output ports of the MZI can be regarded as sequentially appearing refractive index wells for a fixed observation point (see Appendix C). We aim to design the system with the functionality composed of two 50 : 50 couplers and a phase shifter at one of the waveguides in the time domain. The parameters are selected to guarantee that $\kappa_{ij} \approx 0$ in the straight temporal waveguide region in Fig. 3(a), while $\kappa_{ij} \gg 0$ in the curved temporal waveguide region. The additional phase shift φ is realized by an additional change of the refractive index δn for the length 0.4 m corresponding to the red region in Fig. 3(a), resulting in a small change of $\beta_m(z, \tau)$, i.e., the choice of $\delta n/\Delta n \in [0, 1.375 \times 10^{-2}]$ gives effective phase shift $\varphi \in [0, 2\pi]$. We assume the input at port A (port B) as A (B), and the output at port C (port D) as C (D).

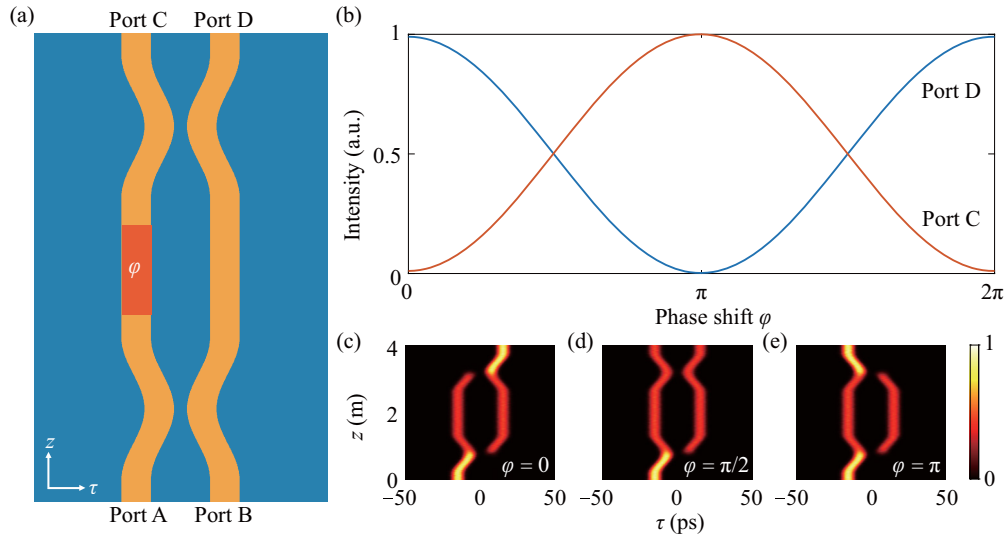


FIG. 3. (a) Schematic of the temporal MZI. (b) Output intensities at port C and port D versus the phase shift δ in simulations based on Eq. (3). (c)–(e) The intensity distributions of the fields for the choice of (c) $\varphi = 0$, (d) $\varphi = \pi/2$, and (e) $\varphi = \pi$.

The relation for a temporal MZI is described by

$$\begin{pmatrix} C \\ D \end{pmatrix} = \begin{pmatrix} \sin \frac{\varphi}{2} & \cos \frac{\varphi}{2} \\ \cos \frac{\varphi}{2} & -\sin \frac{\varphi}{2} \end{pmatrix} \begin{pmatrix} A \\ B \end{pmatrix}, \quad (11)$$

which can be verified by results in our simulation based on Eq. (3) given in Fig. 3(b). In particular, the output at Port C increases as φ increases and reaches its maximum at $\varphi = \pi$ ($\delta n / \Delta n = 6.875 \times 10^{-3}$), while it further decreases and reaches its minimum at $\varphi = 2\pi$ ($\delta n / \Delta n = 1.375 \times 10^{-2}$). The output at port D just behaves exactly in the opposite way. In addition, three specific cases of φ are taken and the intensity distributions of the field are plotted in Figs. 3(c)–3(e). In Fig. 3(c), we inject the pulse at port A, and the pulse gradually switches to the other temporal waveguide during propagation. Such a phenomenon corresponds to a pulse traveling in a spatial waveguide and gradually converting to the other pulse in front of it spatially in the laboratory frame. In Fig. 3(d), the pulse gradually splits into two pulses which correspond to different spatial locations in one spatial waveguide, while in Fig. 3(e), the pulse temporally splits into two pulses, then they converge to the original one eventually.

The proposed temporal MZI could have potential applications in optical signal processing and optical communication. Here, we showcase it being a component of a temporal universal multiport interferometer. The parameters are the same as those used in the above example of MZI. An arbitrary unitary transformation U performed by a temporal universal multiport interferometer with N channels shown in Fig. 4(a) can be decomposed in the following form:

$$U = P \left(\prod_{(m,n) \in S} T_{m,n,l} \right). \quad (12)$$

Here the production follows an ordered sequence (S) of two-channel transformations [27], and

$$T_{m,n,l}(\theta_l, \phi_l) = \begin{pmatrix} 1 & 0 & \dots & \dots & 0 \\ 0 & 1 & & & \\ \vdots & & \ddots & & \vdots \\ & & & e^{i\phi_l} \sin \frac{\theta_l}{2} & \cos \frac{\theta_l}{2} \\ & & & e^{i\phi_l} \cos \frac{\theta_l}{2} & -\sin \frac{\theta_l}{2} \\ \vdots & & & & \ddots & \vdots \\ 0 & & \dots & \dots & & 1 & 0 \\ & & & & & 0 & 1 \end{pmatrix} \quad (13)$$

is the l th transformation in such sequence between two channels m and n ($m = n - 1$), which is realized by a modified MZI with an additional phase shift ϕ_l and splitting parameter θ_l between channels m and n in the time domain as shown in Fig. 4(a). P is a diagonal matrix with complex elements whose modulus are equal to one, corresponding to a phase shift η_m for channel m . We perform a three-channel temporal transformation for the demonstration in principle. $U(n, m)$ is designed as a circulation operator on the three temporal channels as shown in Fig. 4(b). Three pulses with different amplitudes [namely in normalized intensities as 1, 4/9, and 1/9, respectively, shown in Fig. 4(c)] are injected into the input ports. In Fig. 4(c) the pulses take the desired circulation from one temporal waveguide to the other. This result corresponds to sequential-propagating pulses switching their position during propagation in the spatial waveguide in the laboratory frame. In addition, we reconstruct $U(n, m)$ based on the simulation result as shown in Fig. 4(d), which is closely matched with the desired one in Fig. 4(b).

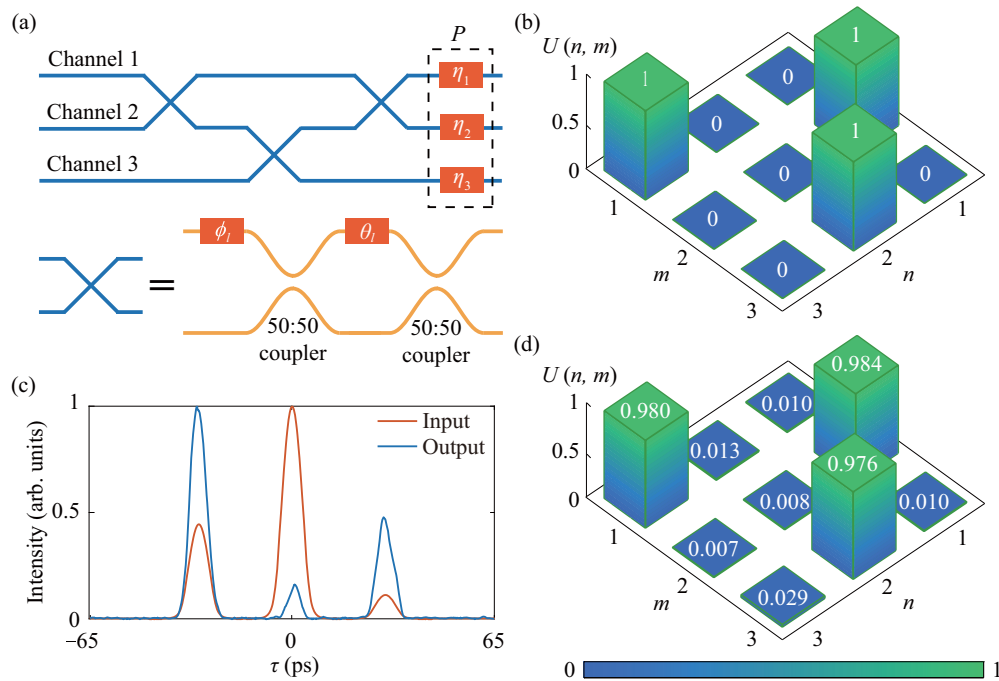


FIG. 4. (a) Schematic of a three-channel temporal universal multiport interferometer. (b) The expected transform matrix $U(n, m)$. (c) Normalized intensities at the input ports and output ports. (d) The reconstructed transform matrix $U(n, m)$ from simulation results. All the simulations are based on Eq. (3).

IV. DISCUSSION AND SUMMARY

We finally make a discussion on the possibility of realizing the proposal in experiments. The parameters in the simulation are achievable with the state-of-art technology in photonics [36–38]. For a pulse with the central wavelength ~ 1000 nm, the corresponding coefficients give $\Delta n \sim 10^{-4}$ and $\beta_2 \sim 10^3$ ps²m⁻¹, which have been demonstrated in experiments [33–35,39]. By properly engineering the waveguide structure, one can further enlarge the group velocity dispersion β_2 [40]. In addition, the synchronization of signal pulses and modulations to precisely control the relative speed between them might be challenging. However, lots of efforts have been made in the field of spatiotemporal photonics [20,41,42]. Very recently, the experimental verification of a single temporal waveguide has been demonstrated [43], which implies the possible demonstration of coupled temporal waveguides in the near future.

In summary, we build a formalism of the temporal coupled-mode equations to study interactions between temporal waveguides in a system where pulses propagate in a spatiotemporally modulated waveguide, and show how systematic parameters of the modulated system determine the temporal coupling coefficients in the theory. One may note that, in temporal photonics, many examples may require simulations beyond the current computational capability of commercial software [44], and hence the assistance of suitable analytical or simplified numerical methods is desired. Our work therefore provides a universal and less computational-costing tool for analyzing spatiotemporally modulated systems. In addition, based on the spatiotemporal coupled-mode equation we developed, a temporal MZI is studied and further, a temporal universal multiport

interferometer in the time domain is proposed, which enables an arbitrary unitary transformation for sequential-propagating pulses. Our work provides a fundamental method, which is useful for optical signal processing in time domain. In particular, compared with the conventional methods with coupled waveguides in the spatial dimension [45–47], the generalization of the coupled temporal waveguides does not require the addition of devices in the space, and the temporal transformation can be performed in only one spatiotemporally modulated waveguide, which greatly reduces the spatial complexity, and insertion loss forms the connection between multiple devices. Moreover, such transformation is realized by the spatiotemporal modulation in an active way, which provides more flexibility in manipulating pulses. The temporal coupled-mode theory in Eqs. (7)–(9) can be further utilized to model two temporal waveguides structure with different systematic parameters and/or modulations that hold complex Δn . In addition, the proposed scheme is also compatible with previous works for controlling a single pulse in one temporal waveguide to achieve pulse compression [48–50], fast and slow light [51–54], and so on [55], hence it can trigger further studies on not only pulse transformation but multifunctional control for pulse propagation with multiple coupled pulse channels in the time domain, which further offers a wealth of opportunities in optical signal processing.

ACKNOWLEDGMENTS

The research was supported by the National Natural Science Foundation of China (Grants No. 12122407, No. 11974245, and No. 12192252), and the National Key Research and Development Program of China

(Grant No. 2021YFA1400900). L.Y. thanks the sponsorship from Yangyang Development Fund and the support from the Program for Professor of Special Appointment (Eastern Scholar) at Shanghai Institutions of Higher Learning.

APPENDIX A: DERIVATION OF EQS. (3) AND (5)

The propagation of the light field along the z direction in a waveguide is described by [56]

$$\nabla^2 \mathbf{E}(\mathbf{r}, t) - \frac{1}{c^2} \frac{\partial^2 \mathbf{E}(\mathbf{r}, t)}{\partial t^2} - \mu_0 \frac{\partial^2 \mathbf{P}(\mathbf{r}, t)}{\partial t^2} = 0, \quad (\text{A1})$$

where $\mathbf{E}(\mathbf{r}, t)$ is the electrical field vector and $\mathbf{P}(\mathbf{r}, t)$ is the polarization. We assume a narrow spectrum width of the light field with a central frequency ω_0 and then apply the slowly varying envelope approximation to separate the rapidly varying part of the electrical field and polarization,

$$\mathbf{E}(\mathbf{r}, t) = \frac{1}{2} \hat{\epsilon} [E(\mathbf{r}, t) \exp(-i\omega_0 t) + \text{c.c.}], \quad (\text{A2a})$$

$$\mathbf{P}(\mathbf{r}, t) = \frac{1}{2} \hat{\epsilon} [P(\mathbf{r}, t) \exp(-i\omega_0 t) + \text{c.c.}], \quad (\text{A2b})$$

where $\hat{\epsilon}$ is the polarization unit vector. By substituting Eq. (A2) into Eq. (A1) and applying the Fourier transformation, we obtain

$$\nabla^2 \tilde{E}(\mathbf{r}, \omega - \omega_0) + \epsilon(\omega) k_0^2 \tilde{E}(\mathbf{r}, \omega - \omega_0) = 0, \quad (\text{A3})$$

where $\tilde{E}(\mathbf{r}, \omega - \omega_0)$ is defined as

$$\tilde{E}(\mathbf{r}, \omega - \omega_0) = \int_{-\infty}^{\infty} E(\mathbf{r}, t) \exp[i(\omega - \omega_0)t] dt, \quad (\text{A4})$$

$\epsilon(\omega)$ is the Fourier transformation of the dielectric constant, and $k_0 = \omega/c$. We assume the solution of Eq. (A3) as

$$\tilde{E}(\mathbf{r}, \omega - \omega_0) = \mathcal{E}(x, y) \tilde{A}(z, \omega - \omega_0) \exp(i\beta_0 z), \quad (\text{A5})$$

where $\tilde{A}(z, \omega - \omega_0)$ is the slowly varying function of z , β_0 is wave number, and $\mathcal{E}(x, y)$ is transverse distribution. Equation (A3) leads to the following equations of $\mathcal{E}(x, y)$ and $\tilde{A}(z, \omega - \omega_0)$ [56]:

$$2i\beta_0 \frac{\partial \tilde{A}}{\partial z} + (\tilde{\beta}^2(\omega) - \beta_0^2) \tilde{A} = 0, \quad (\text{A6a})$$

$$\frac{\partial^2 \mathcal{E}}{\partial x^2} + \frac{\partial^2 \mathcal{E}}{\partial y^2} + [\epsilon(\omega) k_0^2 - \tilde{\beta}^2(\omega)] \mathcal{E} = 0, \quad (\text{A6b})$$

where $\tilde{\beta}(\omega)$ is the Fourier transformation of the wave number and can be determined by Eq. (A6b). We then focus on the solution of \tilde{A} , suppose there is a perturbation of $\tilde{\beta}$ due to a small change of the refractive index, which can be expressed by

$$\tilde{\beta}(\omega) = \beta(\omega) + \beta_m(\omega). \quad (\text{A7})$$

By substituting Eq. (A7) into Eq. (A6a) and using the approximation $\tilde{\beta} + \beta_0 \approx 2\beta_0$, we obtain

$$\frac{\partial \tilde{A}}{\partial z} = i[\beta(\omega) + \beta_m(\omega) - \beta_0] \tilde{A}. \quad (\text{A8})$$

Then using the Taylor expansion of $\beta(\omega)$, we obtain

$$\frac{\partial \tilde{A}}{\partial z} = i \left[\beta_1(\omega - \omega_0) + \frac{\beta_2}{2} (\omega - \omega_0)^2 + \beta(\omega)_m \right] \tilde{A}. \quad (\text{A9})$$

Finally, we use the inverse Fourier transformation to Eq. (A9) then move to the retarded frame to obtain

$$\frac{\partial A(z, \tau)}{\partial z} + \Delta\beta_1 \frac{\partial A(z, \tau)}{\partial \tau} + i \frac{\beta_2}{2} \frac{\partial^2 A(z, \tau)}{\partial \tau^2} = i\beta_m(\tau) A(z, \tau), \quad (\text{A10})$$

which is Eq. (3). We then discuss the solution of Eq. (A10) of the single temporal waveguide case. Since we expect that the $A(z, \tau)$ is an eigenmode of the temporal waveguide without changing its spatiotemporal shape during propagation, we assume

$$A(z, \tau) = M(\tau) \exp[i(Kz - \Omega\tau)]. \quad (\text{A11})$$

By substituting $A(z, \tau)$ into Eq. (A10), we obtain

$$(\Delta\beta_1 + \beta_2\Omega) \frac{\partial M(\tau)}{\partial \tau} = 0, \quad (\text{A12a})$$

$$\frac{\partial^2 M(\tau)}{\partial \tau^2} + \frac{2}{\beta_2} \left[K - \Omega\Delta\beta_1 - \frac{\beta_2\Omega^2}{2} - \beta_m(\tau) \right] M(\tau) = 0. \quad (\text{A12b})$$

To satisfy our assumption, Ω must be taken as $\Omega = -\Delta\beta_1/\beta_2$, and Eq. (A12b) turns to

$$\frac{\partial^2 M(\tau)}{\partial \tau^2} + \frac{2}{\beta_2} \left[K_i + \frac{(\Delta\beta_1)^2}{2\beta_2} - \beta_m(\tau) \right] M(\tau) = 0. \quad (\text{A13})$$

Next, we consider coupled temporal waveguides a and b with the refractive index modulation as Eq. (4). We assume the perturbation due to the other temporal waveguide is small so that the change of spatiotemporal shape $M_i(\tau)$ of the mode in each temporal waveguide can be neglected and only the envelope amplitude of modes in each waveguide changes with the propagation distance [24,57]. We write that the solution $A(z, \tau)$ can be approximated as

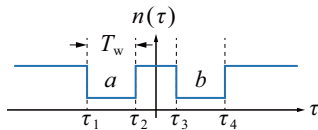
$$A(z, \tau) = G_a(z) M_a(\tau) \exp[i(K_a z - \Omega\tau)] + G_b(z) M_b(\tau) \exp[i(K_b z - \Omega\tau)], \quad (\text{A14})$$

where $M_a(\tau)$ and $M_b(\tau)$ are the normalized modes of the individual temporal waveguides when they are far apart, and $G_i(z)$ denotes the envelope amplitude of the mode in each temporal waveguide. In other words, only $G_i(z)$ is relevant to the amplitude of $A(z, \tau)$ during propagation, and $M_i(\tau)$ plays the role as the transverse modal distribution for spatial waveguide. If the time spacing of the temporal waveguide is infinity, there is no coupling between the two temporal waveguides. $G_a(z)$ and $G_b(z)$ shall be independent on propagation distance z and independent on each other since the two terms of Eq. (A14) satisfy Eq. (A13) separately.

APPENDIX B: SPATIOTEMPORAL FUNDAMENTAL MODES OF A TEMPORAL WAVEGUIDE

In the retarded time frame, the spatiotemporal modes $M(\tau)$ of a temporal waveguide with modulation as

$$\xi(\tau) = \begin{cases} \Delta n_1 & |\tau - \tau_c| \leq T_w/2, \\ \Delta n_2 & |\tau - \tau_c| > T_w/2, \end{cases} \quad (\text{B1})$$


 FIG. 5. $n(\tau)$ of two coupled temporal waveguides.

satisfy Eq. (A13). One finds that Eq. (A13) is similar to the paraxial equation for a spatial waveguide [58]. Therefore, we write a solution similar to the one of a spatial planar waveguide,

$$M(\tau) = \begin{cases} A_1 \cos[\omega_1(\tau - \tau_c) - \phi] & |\tau - \tau_c| \leq T_w/2, \\ A_2 \exp[-\omega_2(|\tau - \tau_c| - T_w/2)] & |\tau - \tau_c| > T_w/2, \end{cases} \quad (\text{B2})$$

where ω_1 and ω_2 are defined as

$$\begin{aligned} \omega_1^2 &= \frac{2K}{\beta_2} + \left(\frac{\Delta\beta_1}{\beta_2}\right)^2 - \frac{2\beta_0\Delta n_1}{n_0\beta_2}, \\ \omega_2^2 &= \frac{2\beta_0\Delta n_2}{n_0\beta_2} - \frac{2K}{\beta_2} - \left(\frac{\Delta\beta_1}{\beta_2}\right)^2. \end{aligned} \quad (\text{B3})$$

The constant A_1 , A_2 , and ϕ can be determined by boundary conditions that both $M(\tau)$ and $dM(\tau)/dt$ are continuous across the boundary. Such boundary conditions lead to the following relation:

$$\omega_2 = \omega_1 \tan(\omega_1 T_w/2 + m\pi/2), \quad (\text{B4})$$

where $m \in \{0, 1, 2, 3, \dots\}$ denotes the mode number. The fundamental mode corresponds to ω_1 and ω_2 satisfying Eq. (3) with $m = 0$.

APPENDIX C: EXPLANATION OF COUPLED TEMPORAL WAVEGUIDES AND INPUT/OUTPUT PORTS

In this section, we explain the coupling between temporal waveguides. In the spatial case, coupling between the two spatial waveguides results from spatial overlap between evanescent tails of the modes in both waveguides at a certain time. Similar things happen in the temporal case too. Although the temporal variation is involved, the spatial evanescent tails still exist as τ depends on both z and t as the two temporal

waveguides are actually two moving refractive index wells. To make this point clear, consider the simplest case of two coupled temporal waveguides with the corresponding $n(\tau)$ being shown in Fig. 5. Since τ depends on both z and t , we can choose a specific t_0 for $n(\tau)$, which reflects the spatial refractive index profile at t_0 . For example, at $t = 0$, the corresponding spatial location where the boundary of temporal waveguide a τ_1 and τ_2 occur are $z_1 = \tau_1 v_B$ and $z_2 = \tau_2 v_B$, respectively. In other words, at $t = 0$, the temporal waveguide a is actually a refractive index well at $z \in [z_1, z_2]$ with a spatial width $T_w v_B$. We then consider how the temporal waveguide changes at $t = dt$. The spatial location where the temporal boundaries τ_1 and τ_2 occur are $z'_1 = dt v_B + \tau_1 v_B$ and $z'_2 = dt v_B + \tau_2 v_B$, respectively. One finds that the temporal waveguide a moves to $z \in [z'_1, z'_2]$ and the moving speed of the temporal waveguide is v_B . Similar analysis can also apply to temporal waveguide b . Therefore, the temporal waveguides a and b are actually two moving refractive index wells in space with a moving speed v_B and the modes in each waveguide is also moving in space as well. As a result, one can find the overlap of the evanescent tails of the modes in space, hence the coupling of the two temporal waveguides can occur. In fact, when the moving speed of temporal waveguides turns to $v_B = 0$, it can return to the common spatial coupling case.

For a more complex case shown in Fig. 3(a), the two channels of the MZI are actually two moving modulation areas with different moving speeds $v_{B,a}$ and $v_{B,b}$ varying with propagation distance, respectively, which forms the curved temporal waveguide region. The ports can be regarded as sequentially appearing refractive index wells in time for an observation point z . We can fix a specific z for $n(\tau)$, which is the temporal variation of refractive index at point z and shows when the temporal waveguide occurs. We take the MZI in Fig. 3(a) as an example. For simplicity, we denote the centers of port A, B, C, and D as τ_A , τ_B , τ_C , and τ_D , respectively. We choose the observation point for the input signals at $z = 0$. One can expect that port A and port B appear sequentially so that the signals at port A and port B can be observed at $t = \tau_A$ and $t = \tau_B$, respectively. Then we choose the observation point for the output signals at $z = L$ [for the MZI shown in Fig. 3(a), $L = 4\text{m}$]. One can observe the output signals at port C and port D at $t = \tau_C + L/v_B$ and $t = \tau_D + L/v_B$, respectively. The input and output ports for the multiport interferometer in Fig. 4(a) can be defined in a similar manner.

-
- [1] N. Engheta, Metamaterials with high degrees of freedom: Space, time, and more, *Nanophotonics* **10**, 639 (2021).
- [2] E. Galiffi, R. Tirole, S. Yin, H. Li, S. Vezzoli, P. A. Huidobro, M. G. Silveirinha, R. Sapienza, A. Alù, and J. Pendry, Photonics of time-varying media, *Adv. Photonics* **4**, 014002 (2022).
- [3] S. Yin, E. Galiffi, and A. Alù, Floquet metamaterials, *eLight* **2**, 8 (2022).
- [4] L. Yuan and S. Fan, Temporal modulation brings metamaterials into new era, *Light Sci. Appl.* **11**, 173 (2022).
- [5] V. Pacheco-Peña, D. M. Solís, and N. Engheta, Time-varying electromagnetic media: Opinion, *Opt. Mater. Express* **12**, 3829 (2022).
- [6] A. M. Shaltout, V. M. Shalae, and M. L. Brongersma, Spatiotemporal light control with active metasurfaces, *Science* **364**, eaat3100 (2019).
- [7] A. Mock, D. Sounas, and A. Alù, Magnet-free circulator based on spatiotemporal modulation of photonic crystal defect cavities, *ACS Photonics* **6**, 2056 (2019).
- [8] Z.-L. Deck-Léger, N. Chamanara, M. Skorobogatiy, M. G. Silveirinha, and C. Caloz, Uniform-velocity spacetime crystals, *Adv. Photonics* **1**, 056002 (2019).
- [9] H. Tian, J. Liu, B. Dong, J. C. Skehan, M. Zervas, T. J. Kippenberg, and S. A. Bhave, Hybrid integrated photonics using bulk acoustic resonators, *Nat. Commun.* **11**, 3073 (2020).

- [10] C. L. Panuski, I. Christen, M. Minkov, C. J. Brabec, S. Trajtenberg-Mills, A. D. Griffiths, J. J. McKendry, G. L. Leake, D. J. Coleman, C. Tran *et al.*, A full degree-of-freedom spatiotemporal light modulator, *Nat. Photon.* **16**, 834 (2022).
- [11] V. Gurses, Enhancing spatiotemporal light modulators, *Nat. Photon.* **16**, 818 (2022).
- [12] E. Galiffi, P. A. Huidobro, and J. B. Pendry, Broadband non-reciprocal amplification in luminal metamaterials, *Phys. Rev. Lett.* **123**, 206101 (2019).
- [13] J. Pendry, E. Galiffi, and P. Huidobro, Gain mechanism in time-dependent media, *Optica* **8**, 636 (2021).
- [14] J. Pendry, E. Galiffi, and P. Huidobro, Gain in time-dependent media—a new mechanism, *J. Opt. Soc. Am. B* **38**, 3360 (2021).
- [15] P. A. Huidobro, E. Galiffi, S. Guenneau, R. V. Craster, and J. B. Pendry, Fresnel drag in space–time-modulated metamaterials, *Proc. Natl. Acad. Sci.* **116**, 24943 (2019).
- [16] L. Xu, G. Xu, J. Huang, and C.-W. Qiu, Diffusive fizeau drag in spatiotemporal thermal metamaterials, *Phys. Rev. Lett.* **128**, 145901 (2022).
- [17] Y. Wang, B. Yousefzadeh, H. Chen, H. Nassar, G. Huang, and C. Daraio, Observation of nonreciprocal wave propagation in a dynamic phononic lattice, *Phys. Rev. Lett.* **121**, 194301 (2018).
- [18] D. L. Sounas and A. Alù, Non-reciprocal photonics based on time modulation, *Nat. Photon.* **11**, 774 (2017).
- [19] S. Taravati, N. Chamanara, and C. Caloz, Nonreciprocal electromagnetic scattering from a periodically space-time modulated slab and application to a quasisonic isolator, *Phys. Rev. B* **96**, 165144 (2017).
- [20] R. Tirole, S. Vezzoli, E. Galiffi, I. Robertson, D. Maurice, B. Tilmann, S. A. Maier, J. B. Pendry, and R. Sapienza, Double-slit time diffraction at optical frequencies, *Nat. Phys.* **19**, 999 (2023).
- [21] B. W. Plansinis, W. R. Donaldson, and G. P. Agrawal, What is the temporal analog of reflection and refraction of optical beams? *Phys. Rev. Lett.* **115**, 183901 (2015).
- [22] B. W. Plansinis, W. R. Donaldson, and G. P. Agrawal, Temporal waveguides for optical pulses, *J. Opt. Soc. Am. B* **33**, 1112 (2016).
- [23] B. W. Plansinis, W. R. Donaldson, and G. P. Agrawal, Cross-phase-modulation-induced temporal reflection and waveguiding of optical pulses, *J. Opt. Soc. Am. B* **35**, 436 (2018).
- [24] H. Haus, *Waves and Fields in Optoelectronics* (Prentice-Hall, Englewood Cliffs, USA, 1984).
- [25] H. A. Haus and W. Huang, Coupled-mode theory, *Proc. IEEE* **79**, 1505 (1991).
- [26] M. Reck, A. Zeilinger, H. J. Bernstein, and P. Bertani, Experimental realization of any discrete unitary operator, *Phys. Rev. Lett.* **73**, 58 (1994).
- [27] W. R. Clements, P. C. Humphreys, B. J. Metcalf, W. S. Kolthammer, and I. A. Walmsley, Optimal design for universal multiport interferometers, *Optica* **3**, 1460 (2016).
- [28] S. Pai, B. Bartlett, O. Solgaard, and D. A. B. Miller, Matrix optimization on universal unitary photonic devices, *Phys. Rev. Appl.* **11**, 064044 (2019).
- [29] W. Bogaerts, D. Pérez, J. Capmany, D. A. Miller, J. Poon, D. Englund, F. Morichetti, and A. Melloni, Programmable photonic circuits, *Nature (London)* **586**, 207 (2020).
- [30] S. Lee, S. Baek, T.-T. Kim, H. Cho, S. Lee, J.-H. Kang, and B. Min, Metamaterials for enhanced optical responses and their application to active control of terahertz waves, *Adv. Mater.* **32**, 2000250 (2020).
- [31] M. A. Gaafar, T. Baba, M. Eich, and A. Y. Petrov, Front-induced transitions, *Nat. Photon.* **13**, 737 (2019).
- [32] W. Cai, Y. Tian, L. Zhang, H. He, J. Zhao, and J. Wang, Reflection and refraction of an airy pulse at a moving temporal boundary, *Ann. Phys.* **532**, 2000295 (2020).
- [33] M. Luennemann, U. Hartwig, G. Panotopoulos, and K. Buse, Electrooptic properties of lithium niobate crystals for extremely high external electric fields, *Appl. Phys. B* **76**, 403 (2003).
- [34] M. Li, J. Ling, Y. He, U. A. Javid, S. Xue, and Q. Lin, Lithium niobate photonic-crystal electro-optic modulator, *Nat. Commun.* **11**, 4123 (2020).
- [35] M. Zhang, C. Wang, P. Kharel, D. Zhu, and M. Lončar, Integrated lithium niobate electro-optic modulators: When performance meets scalability, *Optica* **8**, 652 (2021).
- [36] C. Wang, M. Zhang, X. Chen, M. Bertrand, A. Shams-Ansari, S. Chandrasekhar, P. Winzer, and M. Lončar, Integrated lithium niobate electro-optic modulators operating at cmos-compatible voltages, *Nature (London)* **562**, 101 (2018).
- [37] N. Boynton, H. Cai, M. Gehl, S. Arterburn, C. Dallo, A. Pomerene, A. Starbuck, D. Hood, D. C. Trotter, T. Friedmann *et al.*, A heterogeneously integrated silicon photonic/lithium niobate travelling wave electro-optic modulator, *Opt. Express* **28**, 1868 (2020).
- [38] X. Liu, B. Xiong, C. Sun, J. Wang, Z. Hao, L. Wang, Y. Han, H. Li, and Y. Luo, Sub-terahertz bandwidth capacitively-loaded thin-film lithium niobate electro-optic modulators based on an undercut structure, *Opt. Express* **29**, 41798 (2021).
- [39] A. Kaushalram, S. A. Samad, G. Hegde, and S. Talabattula, Tunable large dispersion in hybrid modes of lithium niobate-on-insulator multimode waveguides, *IEEE Photon. J.* **11**, 1 (2019).
- [40] L. Zhang, Y. Yue, Y. Xiao-Li, R. G. Beausoleil, and A. E. Willner, Highly dispersive slot waveguides, *Opt. Express* **17**, 7095 (2009).
- [41] C. Liang, S. A. Ponomarenko, F. Wang, and Y. Cai, Temporal boundary solitons and extreme superthermal light statistics, *Phys. Rev. Lett.* **127**, 053901 (2021).
- [42] O. Segal, E. Lustig, S. Saha, E. Bordo, S. N. Chowdhury, M.-I. Cohen, A. Fleischer, M. Ozlu, A. Boltasseva, O. Cohen *et al.*, Time-refraction with moving time-interfaces, in *CLEO: Fundamental Science* (Optica Publishing Group, San Jose, USA, 2023), pp. FTu3D–2.
- [43] J. Zhang, W. Donaldson, and G. P. Agrawal, Experimental observation of a raman-induced temporal waveguide, *Phys. Rev. A* **107**, 063518 (2023).
- [44] Y. Shi, W. Shin, and S. Fan, Multi-frequency finite-difference frequency-domain algorithm for active nanophotonic device simulations, *Optica* **3**, 1256 (2016).
- [45] S. Kawanishi, Ultrahigh-speed optical time-division-multiplexed transmission technology based on optical signal processing, *IEEE J. Quantum Electron.* **34**, 2064 (1998).
- [46] S. A. Hamilton, B. S. Robinson, T. E. Murphy, S. J. Savage, and E. P. Ippen, 100 gb/s optical time-division multiplexed networks, *J. Lightwave Technol.* **20**, 2086 (2002).
- [47] D. A. Miller, Self-configuring universal linear optical component, *Photonics Res.* **1**, 1 (2013).

- [48] A. T. Ryan and G. P. Agrawal, Pulse compression and spatial phase modulation in normally dispersive nonlinear kerr media, *Opt. Lett.* **20**, 306 (1995).
- [49] N. L. Wagner, E. A. Gibson, T. Popmintchev, I. P. Christov, M. M. Murnane, and H. C. Kapteyn, Self-compression of ultrashort pulses through ionization-induced spatiotemporal reshaping, *Phys. Rev. Lett.* **93**, 173902 (2004).
- [50] N. Chamanara, D. G. Cooke, and C. Caloz, Linear pulse compression based on space-time modulation, in *2019 IEEE International Symposium on Antennas and Propagation and USNC-URSI Radio Science Meeting* (IEEE, Atlanta, USA, 2019), pp. 239–240.
- [51] P. Kolchin, C. Belthangady, S. Du, G. Y. Yin, and S. E. Harris, Electro-optic modulation of single photons, *Phys. Rev. Lett.* **101**, 103601 (2008).
- [52] L. Thévenaz, Slow and fast light in optical fibres, *Nat. Photon.* **2**, 474 (2008).
- [53] R. W. Boyd, Slow and fast light: Fundamentals and applications, *J. Mod. Opt.* **56**, 1908 (2009).
- [54] G. Li, Y. Chen, H. Jiang, X. Liu, X. Chen *et al.*, Tunable temporal gap based on simultaneous fast and slow light in electro-optic photonic crystals, *Opt. Express* **23**, 18345 (2015).
- [55] G. Li, D. Yu, L. Yuan, and X. Chen, Single pulse manipulations in synthetic time-frequency space, *Laser Photonics Rev.* **16**, 2100340 (2022).
- [56] G. P. Agrawal, *Nonlinear Fiber Optics*, 5th ed. (Academic Press, Boston, USA, 2013).
- [57] A. Yariv and P. Yeh, *Photonics: Optical Electronics in Modern Communications*, 6th ed. (Oxford University Press, Oxford, USA, 2007).
- [58] G. P. Agrawal, *Lightwave Technology: Components and Devices* (John Wiley & Sons, Hoboken, USA, 2004).